

The secular planetary three body problem revisited

Jacques Henrard and Anne-Sophie Libert

Département de mathématique FUNDP, 8, Rempart de la Vierge, B-5000 Namur, Belgique
e-mail: jacques.henrard@fundp.ac.be

Abstract. We analyze the secular interactions of two coplanar planets based on a high order (order 12) expansion of the perturbative potential in powers of the eccentricities. The model depends on only two parameters (the ratio of semi-major axis and the mass ratio of the planets) and can be reduced to a one degree of freedom system, allowing for an exhaustive parametric analysis. Following Pauwels (1984) we map the phase space on a sphere, avoiding in this way the artificial singularities introduced by other mappings. We show that the twelve order expansion is able to describe correctly most of the exosolar planetary systems discovered so far, even if the eccentricities of these planets are considerably larger than the eccentricities of our own solar system. The expansion is even able to reproduce, at moderate eccentricities, the secular resonances discovered numerically by Michtchenko and Malhotra (2004) at moderate to large eccentricities.

Keywords. Secular planetary problem, high order expansions, exosolar planetary systems

1. Introduction

The number of discovered exoplanets is growing fast. A few of them, but their number is also growing, form genuine planetary systems, being planets of the same star. Due possibly to observational bias, these systems are quite different from our own planetary system: large planetary masses, very large eccentricities are common. Some of the pairs of planets are locked in a mean motion resonance and their orbits are significantly perturbed; but even in the non-resonant case, long term secular effects may produce interesting dynamical phenomena and large amplitude variation of eccentricities.

Due to the large values of the eccentricities, the applicability of the classical Laplace-Lagrange linear perturbation theory is very limited. But it is worth investigating if a *non-linear* analytical theory, based on a high order expansion of the secular perturbation may not be applicable, at least for some of the discovered systems.

This is the aim of this contribution. We expand the secular interactions of a couple of coplanar planets up to order 12 in the eccentricities, and check that this expansion modelizes correctly several of the observed systems. The analytical modelization, valid not only for low, but for moderately high eccentricity, facilitates the parametric analysis of the secular interaction of a couple of planets. Essentially, two parameters are involved, the ratio $\alpha = a_1/a_2$ of the semi-major axis and the mass ratio $\mu = m_1/(m_1 + m_2)$. We restrict ourself to planar systems because no or very little information on inclination is available, but, of course, a similar analytical modelization of inclined systems is possible although its analysis would be more involved.

To describe the phase space of the problem we use the representation introduced by Pauwels (1983) which is free of the artificial singularities which mar the traditional representations. We believe that, with this representation, the phase-space diagrams are simpler and much more readable.

As a further indication of the interest of our analytical approach, we reproduce, at moderate eccentricities, the numerical results of Michtchenko and Malhotra (2004) concerning the existence of a secular resonance at moderate to large eccentricities.

2. The Planar Secular Three Body Problem

Let us consider a central star of mass m_0 and two coplanar planets of mass m_1 and m_2 . Using the usual Jacobi coordinates the Hamiltonian of the dynamics of this system is (up to the second powers in the mass ratios m_1/m_0 and m_2/m_0)

$$\mathcal{H} = -\frac{Gm_0m_1}{2a_1} - \frac{Gm_0m_2}{2a_2} - Gm_1m_2 \left[\frac{1}{|\vec{r}_1 - \vec{r}_2|} - \frac{(\vec{r}_1|\vec{r}_2)}{r_2^3} \right] \tag{2.1}$$

where a_i , \vec{r}_i and r_i are, respectively, the osculating semi-major axis, the position vector and the norm of the position vector of the mass m_i (see for instance Brouwer and Clemence 1961 or Laskar, 1990). We assume that the mass m_1 is the one closest to the central star. To the second order in the mass ratios, the classical modified Delaunay's elements (see references above) are:

$$\begin{aligned} \lambda_i &= \text{mean longitude of } m_i & L_i &= m_i \sqrt{Gm_0 a_i} \\ p_i &= - \text{the longitude of the pericenter of } m_i & P_i &= L_i [1 - \sqrt{1 - e_i^2}]. \end{aligned} \tag{2.2}$$

The perturbation (the last term in equation (2.1), can be expanded in powers of the eccentricities (see for instance Murray and Dermott 1999) to yield:

$$\begin{aligned} \mathcal{H} = & -\frac{Gm_0m_1}{2a_1} - \frac{Gm_0m_2}{2a_2} \\ & - \frac{Gm_1m_2}{a_2} \sum_{k,i_1,i_2,j_1,j_2} A_{i_1,i_2,j_1,j_2}^k e_1^{|j_1|+2i_1} e_2^{|j_2|+2i_2} \cos \Phi, \end{aligned} \tag{2.3}$$

where $\Phi = [(k + j_1)\lambda_1 - (k + j_2)\lambda_2 + j_1p_1 - j_2p_2]$. The coefficients A_{i_1,i_2,j_1,j_2}^k depend only on the ratio a_1/a_2 of the semi-major axis. As we plan to use extensively the canonical variables defined in (2.2), we prefer to use the expressions $E_i = \sqrt{2P_i/L_i}$ rather than e_i . Notice that for small to moderate eccentricities $E_i \approx e_i$. Hence the Hamiltonian reads:

$$\begin{aligned} \mathcal{H} = & -\frac{Gm_0m_1}{2a_1} - \frac{Gm_0m_2}{2a_2} \\ & - \frac{Gm_1m_2}{a_2} \sum_{k,i_1,i_2,j_1,j_2} B_{i_1,i_2,j_1,j_2}^k E_1^{|j_1|+2i_1} E_2^{|j_2|+2i_2} \cos \Phi. \end{aligned} \tag{2.4}$$

As we are interested in the long term dynamics and as we assume that we are not close to a mean motion commensurability, we average the Hamiltonian function over the “fast variables” λ_i . To the first order in the mass ratios, the averaging amount to a “averaging by scissors” (dropping the fast periodic terms from the function). We are left with:

$$\mathcal{K} = -\frac{Gm_0m_1}{2a_1} - \frac{Gm_0m_2}{2a_2} - \frac{Gm_1m_2}{a_2} \sum_{k,i_1,i_2} C_{i_1,i_2}^k E_1^{k+2i_1} E_2^{k+2i_2} \cos k(p_1 - p_2), \tag{2.5}$$

where a_i , E_i and p_i designate now averaged values. The “fast variables” λ_i are now ignorable which means that the L_i and thus the a_i are constant. The first two terms of (2.5), being constant, can be dropped from the Hamiltonian. Also the Hamiltonian depends only on the difference $(p_1 - p_2)$; hence the sum $P_1 + P_2$ is a first integral of the problem which can be reduced to one degree of freedom.

Before analyzing further this simplified model, it is useful to check whether it may be applied to exosolar systems. The eccentricity of many of the observed exoplanets is rather high and one may wonder if the above expansion in powers of the eccentricities can represent their orbits with enough accuracy. We have computed the expansion (up to order 12) for several of the exosystems of planets and report the numerical convergence in Table I.

Table I: Convergence of the expansion (2.5) for some exosystems.

	(c-d) v And.	Gliese 876	HD168443	HD169830	HD37124
α	0.332	0.62	0.10	0.22	0.22
μ	0.335	0.23	0.30	0.42	0.38
e_1	0.28	0.10	0.53	0.31	0.10
e_2	0.27	0.27	0.23	0.33	0.69
$p_1 - p_2$	-10°	3°	110°	-104°	-200°
ord. 2	$5.9 \cdot 10^{-3}$	$1.4 \cdot 10^{-2}$	$7.8 \cdot 10^{-4}$	$7.3 \cdot 10^{-3}$	$7.5 \cdot 10^{-3}$
ord. 4	$4.7 \cdot 10^{-4}$	$-2.5 \cdot 10^{-4}$	$-1.2 \cdot 10^{-5}$	$2.4 \cdot 10^{-3}$	$3.1 \cdot 10^{-3}$
ord. 6	$2.8 \cdot 10^{-5}$	$-3.6 \cdot 10^{-6}$	$-6.1 \cdot 10^{-7}$	$7.1 \cdot 10^{-4}$	$1.1 \cdot 10^{-3}$
ord. 8	$1.4 \cdot 10^{-6}$	$5.9 \cdot 10^{-8}$	$-1.2 \cdot 10^{-8}$	$2.0 \cdot 10^{-4}$	$3.8 \cdot 10^{-4}$
ord. 10	$7.2 \cdot 10^{-8}$	$1.8 \cdot 10^{-9}$	$-1.4 \cdot 10^{-10}$	$5.9 \cdot 10^{-5}$	$1.4 \cdot 10^{-4}$
ord. 12	$3.8 \cdot 10^{-9}$	$-1.4 \cdot 10^{-11}$	$-4.4 \cdot 10^{-13}$	$1.8 \cdot 10^{-5}$	$5.0 \cdot 10^{-5}$

Listed in Table I are the physical parameters of the systems: $\alpha = a_1/a_2$ the ratio of semi-major axis, $\mu = m_1/(m_1 + m_2)$, the mass ratio, the eccentricities of the two components of the systems and the contributions to the value of the Hamiltonian, from order 2 to order 12 in E_1 and E_2 , of the terms in the expansion (2.5). The numerical convergence is excellent for the first three systems, marginal for the last two.

3. Reduction to One Degree of Freedom and Display of the Phase Space

In order to bring forward the fact that the problem may be reduced to a one degree of freedom problem, it is enough to introduce the new canonical variables:

$$\begin{aligned}
 u = p_2 & \quad ; \quad U = (P_1 + P_2)/[(m_1 + m_2)\sqrt{Gm_0a_2}] \\
 v = p_1 - p_2 & \quad ; \quad V = P_1/[(m_1 + m_2)\sqrt{Gm_0a_2}].
 \end{aligned}
 \tag{3.1}$$

We have introduced the factor $(m_1 + m_2)\sqrt{Gm_0a_2}$ in order to make non dimensional the new actions U and V . Notice that the constant U is a weighted mean of the square of the two eccentricities when they are small:

$$U = \mu\sqrt{\alpha} \left[1 - \sqrt{1 - e_1^2} \right] + (1 - \mu) \left[1 - \sqrt{1 - e_2^2} \right].
 \tag{3.2}$$

Up to a constant (the first two terms of (2.5)) and to a factor (the factor $-Gm_1m_2/a_2$), which can be absorbed by redefining the time scale, the Hamiltonian reads

$$\mathcal{K}^* = \sum_{n \geq 1} U^n \sum_{k=0}^n \sum_{i_1=0}^{n-k} C_{i_1, i_2}^k \left[\frac{2V}{U\mu\sqrt{\alpha}} \right]^{(k+2i_1)/2} \left[\frac{2(U - V)}{U(1 - \mu)} \right]^{(k+2i_2)/2} \cos kv,
 \tag{3.3}$$

where $i_2 = n - k - i_1$. The quantity U being a constant, the trajectories of the one

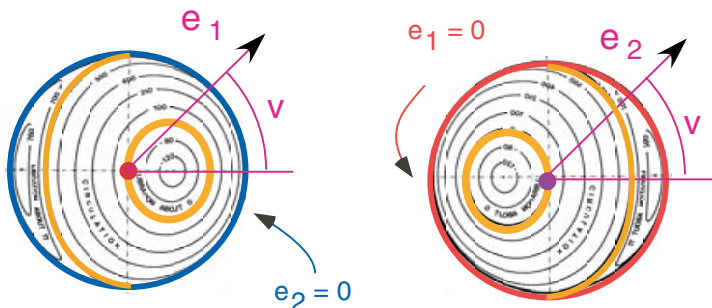


Figure 1. The usual representation of the level curves of the Hamiltonian (3.3) on a plane parametrized by polar coordinates with one of the eccentricities as distance and the difference in longitude of the pericenter as angular variables. The drawback of this representation is that the outer circle represents a single point; a fact that introduces artificial singularities.

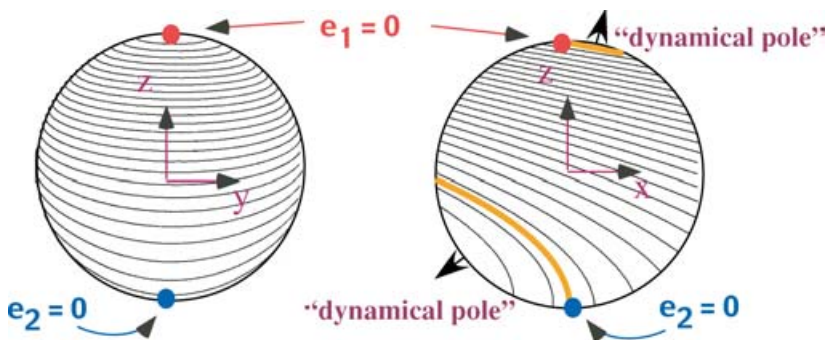


Figure 2. The projection on the $[x, z]$ and the $[y, z]$ plane of the Pauwel's sphere. The thick curves are the ones passing through the geographical poles (where one of the eccentricities vanishes). In the traditional representation they are singular, but nothing set them apart in this representation of the phase space.

degree of freedom system, (v, V) , are the level curves of the Hamiltonian function on a two dimensional manifold. Usually the level curves are drawn on a plane the polar coordinates of which are v and e_1 or v and e_2 (see Figure 1). The fact that the outer circles correspond to a single point ($e_1 = 0$ to the left, $e_2 = 0$ to the right) introduces uncalled for artificial singularities in the problem and makes difficult the interpretation of the figures.

We much prefer to use the representation of the manifold $U = \text{constant}$ introduced by Pauwels (1983). Let us define an angle ϕ by the equation:

$$\frac{P_1}{P_1 + P_2} = \frac{V}{U} = \frac{1}{2}[1 - \sin \phi]. \tag{3.4}$$

As V/U belongs to the interval $[0, 1]$ ($V/U = 0$ when $e_1 = 0$ and $V/U = 1$ when $e_2 = 0$), the angle ϕ belongs to the interval $[-\pi/2, \pi/2]$. At the extreme values the angular variable $v = p_1 - p_2$ is undefined. Hence the phase space has the topology of a sphere with ϕ as latitude and v as longitude. The particular values $e_1 = 0$ and $e_2 = 0$ represent the poles of this sphere. Of course it is not as easy to draw level curves on a sphere than on a plane, but we believe that the projections of the sphere on some plane (we have chosen, in Figure 2, the $[x, z]$ plane and the $[y, z]$) is informative enough. The really interesting points are the equilibria which we call *dynamical poles*.

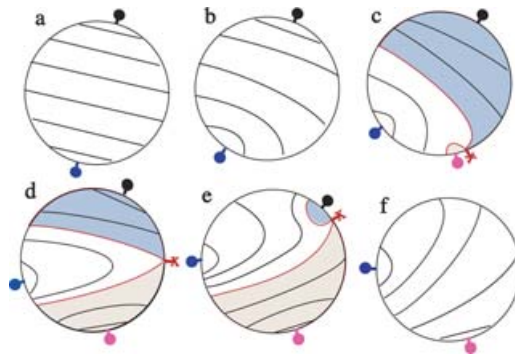


Figure 3. The projection on the $[x, z]$ plane of the Pauwel's spheres for $\alpha = 0.166$ and $m_1/m_2 = 1$. From (a) to (f) the constant U , and thus the weighted mean eccentricity, increases. The secular resonance appears from (c) to (e) – from $U = 0.12$ and $U = 0.151$. See the text for further comments.

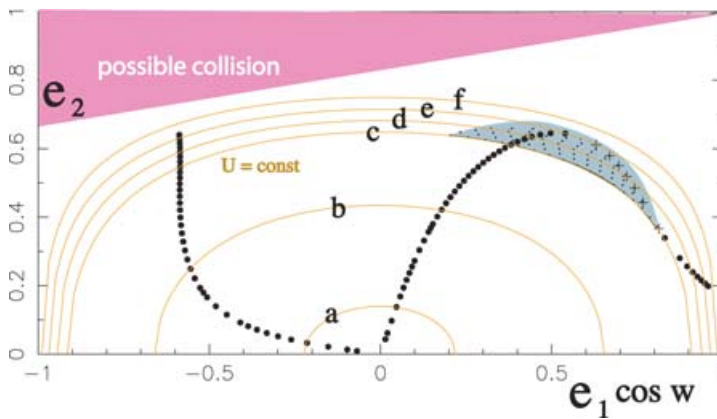


Figure 4. The singular points on the Pauwel's sphere for $\alpha = 0.166$ and $m_1/m_2 = 1$. The right half of this plane (the part with $\cos w = 1$) should be compared with the lower left panel of Figure 8 of Michtchenko and Malhotra paper (2004). See the text for further comments.

4. The Non-Linear Resonance of the Planar Secular Planetary Three-Body Problem

Michtchenko and Malhotra (2004) have shown recently that there exists, at moderate-to-high eccentricity, a secular resonance between the motion of the pericenter of the two planets. Their results are based on a semi-numerical approach which employs a numerical averaging of the short period interactions of the planets and a subsequent numerical integration of the averaged differential equations. It is a challenge for our analytical approach to reproduce at least part of their results. Of course we are unable to reproduce them when they appear at very high eccentricities; but, as shown in Figures 3 and 4, the analytical modelization is able to detect and describe correctly the secular resonance when it appears at moderate eccentricity. In that case, the analytical approach leads to a much easier analysis. The Hamiltonian function and its derivatives are rather simple functions of the spherical coordinates (ϕ, v) . Trajectories are level curves of \mathcal{K}^* ; equilibria are roots of a simple polynomial; maximum and minimum values of the eccentricities along a trajectory are easily computed, etc.

Figure 3 shows, for $\alpha = a_1/a_2 = 0.166$ and $\mu = m_1/(m_1 + m_2) = 0.5$, the evolution of the phase space when the parameter U increases. For $U = 0.005$ (Figure 3a) the

dynamical problem is almost linear and the level curves are almost circles centered on a line $(y, z) = (\sin \beta, \cos \beta)$. Actually, for the linear problem obtained by keeping only the quadratic terms in the expansion of the Hamiltonian, a rotation of the sphere by the angle β (which is a simple function of the parameters α and μ) maps the level curves on the lines of constant latitude. The poles of this transformed sphere are the equilibria. This is the reason why we have called them *dynamical poles*, in contrast to the *geometrical poles* which correspond to the phases $e_1 = 0$ and $e_2 = 0$.

For $U = 0.05$, the southern dynamical pole goes toward the geometrical equator much faster than the northern dynamical pole and the level curves are distorted. For a value of U slightly smaller than 0.12 a cusp appears on one of the level curves and for $U = 0.12$ (see Figure 3c) a small loop is created containing a third equilibrium. An unstable equilibrium generates two homoclinic orbits which divide the sphere in three domains associated each with one of the equilibria. For larger values of U (see Figure 3d for $U = 0.135$) the small loop grows and the domain associated with the northern pole shrinks. At $U = 0.151$ (see Figure 3e) this domain is reduced to a small loop surrounded by one of the homoclinic orbits. For a slightly larger value of U this dynamical pole and the unstable equilibrium merge and disappear. For larger values (see Figure 3f for $U = 0.17$), the topology of the phase space is the same as before the apparition of the equilibrium. The sphere is undivided by homoclinic orbits. What was the northern dynamical pole has disappeared,; what was the southern dynamical pole has moved in the northern hemisphere and the third equilibrium, promoted to the role of a dynamical pole, has taken a position close to the southern geometric pole (i.e. for $e_2 \approx 0$).

Figure 4 summarize the location of the dynamical poles on the circles $y = 0$ of the Pauwel's spheres. For the value of U of each of the sphere of Figure 3, the curve $U = \text{constant}$ is drawn in the plane e_1, e_2 . Notice that in order to distinguish between the left and right sides of the maps in Figure 3, we attribute a negative value to e_1 when x is negative or equivalently when $v = \pi$. Dots indicate the position of dynamical poles (stable equilibria). Between $U = 0.12$ and $U = 0.151$ they are three of them. A cross indicates the position of the unstable equilibria responsible for the homoclinic trajectories which divide the spheres in three domains. Small dots indicates the extend of the secular resonance (dark areas in Figure 3). The right half of Figure 4 reproduce almost exactly the lower left panel of Figure 8 of Michtchenko and Malhotra (2004) paper.

References

- Brouwer, D. and Clemence, G.M 1961, *Methods of Celestial Mechanics*, Academic Press
- Laskar, J. 1990, in: D. Benest and C. Froeschlé (eds.), *Les méthodes modernes de la mécanique céleste*, Editions Frontière, p. 63
- Michtchenko, T.A. and Malhotra, R. 2004, *Icarus*, 168, 237
- Murray, C.D. and Dermott, S.F. 1999, *Solar System Dynamics*, Cambridge Univ. Press
- Pauwels, T. 1983, *Celest. Mech.*, 30, 229